Ghiasvand et al. International Journal of Mechanical and Materials Engineering (2020) 15:6
https://doi.org/10.1186/s40712-020-00118-y

International Journal of Mechanical and Materials Engineering

ORIGINAL PAPER Open Access

Effects of tool offset, pin offset, and alloys position on maximum temperature in dissimilar FSW of AA6061 and AA5086

Amir Ghiasvand[1], Mahdi Kazemi[2*], Maziar Mahdipour Jalilian[3] and Hossein Ahmadi Rashid[1]

Abstract

Friction stir welding (FSW) is a solid-state welding technique, which two workpieces join by pressure and large plastic deformation near their melting points. The tool offset, pin offset, and position of dissimilar alloys can highly affect the maximum temperature and heat distribution in FSW process. In current research, the effects of three mentioned variables on the maximum temperature of FSW of AA6061 and AA5086 alloys have been investigated. In this manner, Response Surface Methodology (RSM) as an auxiliary method has been used. The results show that pin offset is the most effective parameter affecting maximum achieved temperature. In all pin and tool offsettings, placing the harder alloy (AA6061) at advancing side results in more maximum temperature increment compared to the case which the harder alloy is at the retreating side.

Keywords: Friction stir welding, Tool offset, Pin offset, Maximum temperature, Aluminum alloys, Response surface method

Introduction

Friction stir welding (FSW) is a solid-state welding technique, which two workpieces join by pressure and large plastic deformation near their melting points (Mishra et al., 2014). In comparison with other techniques, FSW has some advantages, e.g., lower required energy, lower residual stress, better mechanical properties, lower defects, and nature-friendly (Aliha et al., 2016). This process is used to join similar and dissimilar materials. The main factor in forming appropriate and defectless connection in the FSW process is generating heat and its proper distribution. Heat in FSW is generated by friction and plastic flow (Schmidt et al., 2003). Friction between tool and workpiece generates the most fraction of required heat (Mishra et al., 2014). Due to asymmetrical heat distribution in FSW, different regions are formed in workpieces. These regions are highly different from each other because of different plastic deformations, heat distributions, residual stresses, and microstructures. In FS welding of dissimilar materials, controlling the heat distribution is very important due to different mechanical and thermal properties of materials, which causes to intense asymmetry of heat distribution at joints. To avoid this disadvantage, one must offset tool from the weld line (Yaduwanshi et al., 2018). As a new method, offsetting pin from shoulder can be used to achieve normal heat distribution in workpieces (Essa et al., 2016). Offsetting the pin causes increment in plastic material flow in a constant pin volume, which leads to increase the area of welded cross section.

Many researches have been performed on tool offsetting. Ramachandran et al. (Ramachandran et al., 2015) studied the effect of tool offset distance on mechanical properties and microstructures of HSLA steel—as retreating side—and AA5052-H32 aluminum alloy friction stir welding. The results show that offset distance can affect the mechanical properties and

* Correspondence: kazemi@malayeru.ac.ir; kazemii.m@gmail.com
[2]Department of Mechanical Engineering, Faculty of Engineering, Malayer University, Malayer, Iran
Full list of author information is available at the end of the article

microstructures intensely. Khan et al. (Khan et al., 2015) investigated the effect of tool offset distance and shoulder penetration on defects in FSW process of AA5083-H116—as advancing side—and AA6063-T6. They found that offsetting toward the more ductile side avoids tunnel defects and leads to significant increment in ultimate tensile strength (UTS). Shah et al. (Shah et al., 2018) studied the effect of tool eccentricity on material flow in FSW process of AA6061 and found that offsetting increases the material flow and weld area. Naghibi et al. (Naghibi et al., 2016) investigated the influence of tool offset on the UTS of AA5052 and AISI 304 weld joint and optimized UTS by genetic algorithm. Liang et al. (Liang et al., 2013) studied the effects of process parameters and tool offset on the mechanical properties of weld joint of aluminum and magnesium—as advancing side—alloys. In regard to their research, in all rotational speeds, offsetting toward either aluminum or magnesium alloy leads to decrement in UTS. Sahu et al. (Sahu et al., 2016)investigated the effective variables in FSW of two dissimilar metals copper and aluminum. The results showed that in an optimized offset value and placing aluminum as advancing side, the maximum joint quality was achieved. Pandia and Menghani (Pandya & Menghani, 2018) studied the effect of offsetting in FSW of AA6061-T6 and copper—as advancing side—and found that the best mechanical properties are achieved at 1 mm of offset. Kar et al. (Kar et al., 2019) investigated the effect of offsetting on material flow in FSW of aluminum and titanium. It was found that offsetting intensely increases the material flow. Mastanaiah et al. (Mastanaiah et al., 2016) studied the effects of process parameters and tool offset on defects forming in FSW of AA5083 and AA2219. The results showed that tool offset could affect the weld mechanical properties. Tamjidi et al. (Tamjidy et al., 2017) optimized the mechanical properties of joint made by FSW of AA6061—as advancing side—and AA7075 by investigating the tool offset effect. Mehta and Badheka (Mehta & Badheka, 2015) investigated the effect of tool offset and geometry on mechanical properties of AA6061 and copper—as advancing side—weld joint and found the optimized value of tool offset. Rasaee et al. (Rasaee et al., 2018) studied the effect of tool offset on mechanical properties of weld joint of AA6061 and copper—as advancing side. They found that at 1 mm offset toward the copper, the maximum UTS is achieved. There are a few researches on pin offsetting. Mao et al. (Mao et al., 2014) studied four different pin offsets in FSW of AA7075 and found the optimum offset which causes weld area increment and microstructure and mechanical properties improvement. Amini et al. (Amini et al., 2015) investigated the effect of pin geometry on mechanical properties of FSW of AA5083. The results indicated that using a pin with the offset of 1.5 mm results in increment in plastic flow, elongation, and UTS.

In addition to mentioned parameters (tool offset and pin offset), material position affects the joint mechanical properties, temperature distribution, and plastic flow. Due to asymmetry of plastic flow on both sides of the welding line, material position plays a great role on temperature distribution, mechanical properties, and microstructure of joint (Shah et al., 2019). Many works have been performed on FSW of dissimilar metals but the effect of material position on temperature distribution and maximum temperature has been almost neglected.

In this research, the effects of pin offset, tool offset, and alloys position in dissimilar FSW of AA6061 and AA5086 aluminum alloys on process temperature have been studied simultaneously using experimental and numerical methods which have not been performed yet. To investigate the effects of three mentioned variables on the maximum temperature of process and find their interactions, Response Surface Methodology (RSM) has been used.

Experimental procedure

In current study, two dissimilar aluminum alloys, AA6061-T6 (harder alloy), and AA5086-O were used to perform FSW process, which their chemical compositions have been illustrated in Table 1. In this way, two workpieces with dimensions of 120 × 50 × 5 mm^3 were prepared for welding.

In all experiments, AA6061-T6 alloy was placed at advancing side. Rotational speed, travel speed, and tilt angle of tool were considered as 840 rpm, 150 mm/min, and 0°, respectively. The schematic of FSW process has been shown in Fig. 1.

To study the effect of pin offsetting on heat distribution and temperature history, five tools with different

Table 1 Chemical compositions of used alloys (wt%)

Aluminum alloy	Mg	Mn	Cu	Cr	Si	FE	AL
AA6061-T6	0.918	0.083	0.328	0.065	0.663	0.491	Balance
AA5086-O	4.12	0.447	0.031	0.105	0.244	0.343	Balance

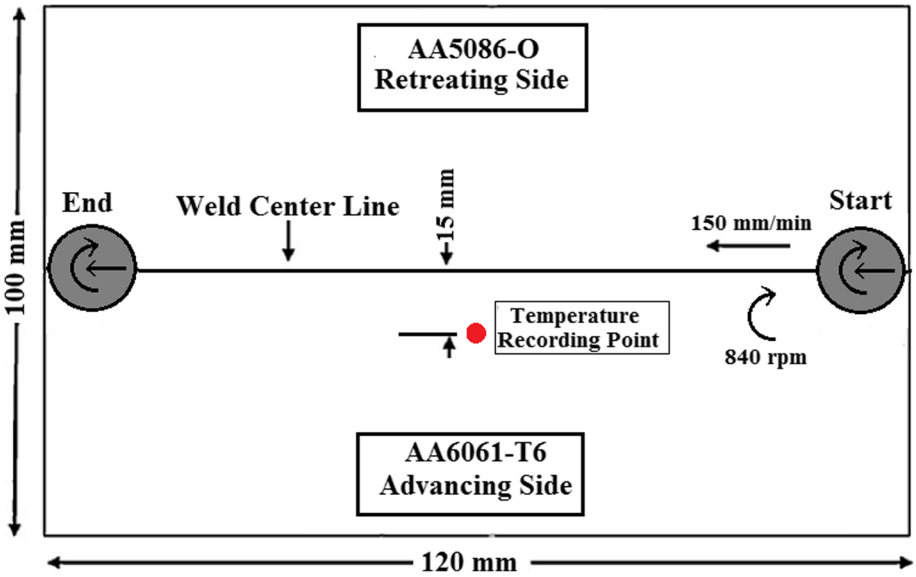

Fig. 1 The schematic of FSW process

pin offsets were used. Heat-treating steel H13 was utilized to produce the tools. After that, tools experienced heat-treated hardening to increase the hardness and corrosion resistance. It should be mentioned that the surface roughness of pins and shoulders was negligible. Tools and their relevant dimensions have been illustrated in Fig. 2 and Table 2, respectively.

To perform the FSW process, milling machine was utilized and after production of proper fixture, five cases were investigated. To record the temperature of welded specimens, infra-red thermometer was fixed on the moving part of the milling machine to move with the speed equal to FSW travel speed. During the each FSW process, temperature history of a point

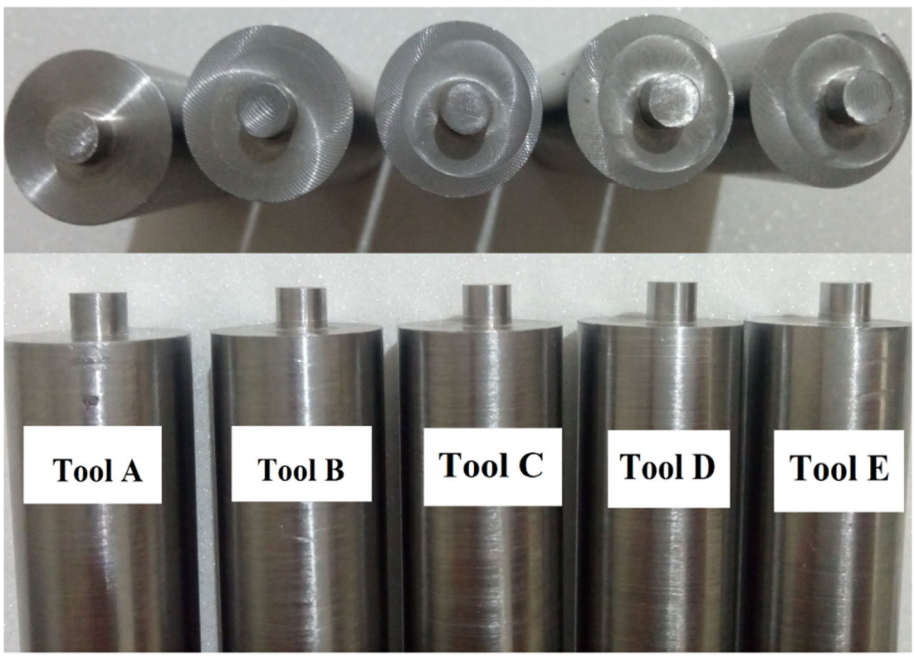

Fig. 2 Used tools in experiments

Table 2 Dimensions of tools

Tool	Shoulder diameter (mm)	Pin diameter (mm)	Pin length (mm	Pin offset (mm
A	20	6	4.7	0
B	20	6	4.7	0.5
C	20	6	4.7	1
D	20	6	4.7	1.5
E	20	6	4.7	2

located at the distance of 15 mm of weld line of advancing side (based on Fig. 1) was recorded. The weld apparatus and thermometer have been shown in Fig. 3. Also, welded specimens with five different tools have been illustrated in Fig. 4.

Finite elements modeling

There are various methods to model the FSW process with their specific advantages and disadvantages (Meyghani et al., 2017). Coupled Eulerian-Lagrangian (CEL) approach is the method of using Eulerian and Lagrangian elements simultaneously (Al-Badour et al., 2013). The tool was modeled using this method. Using this method, one can study the effect of tool geometry on the welding process. In this research, numerical simulation of FSW process has been performed using the CEL approach.

To verify the numerical simulation process, in first step, five experimental temperature histories were used. Numerical model specifications were selected as

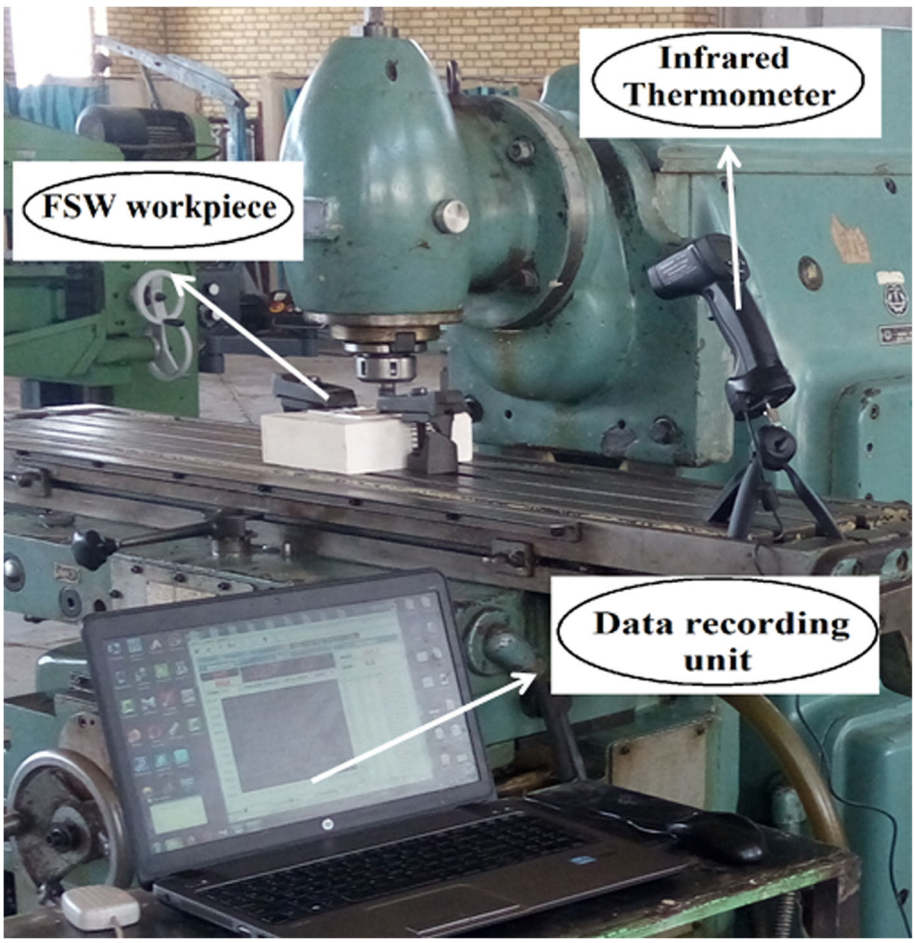

Fig. 3 FSW set-up

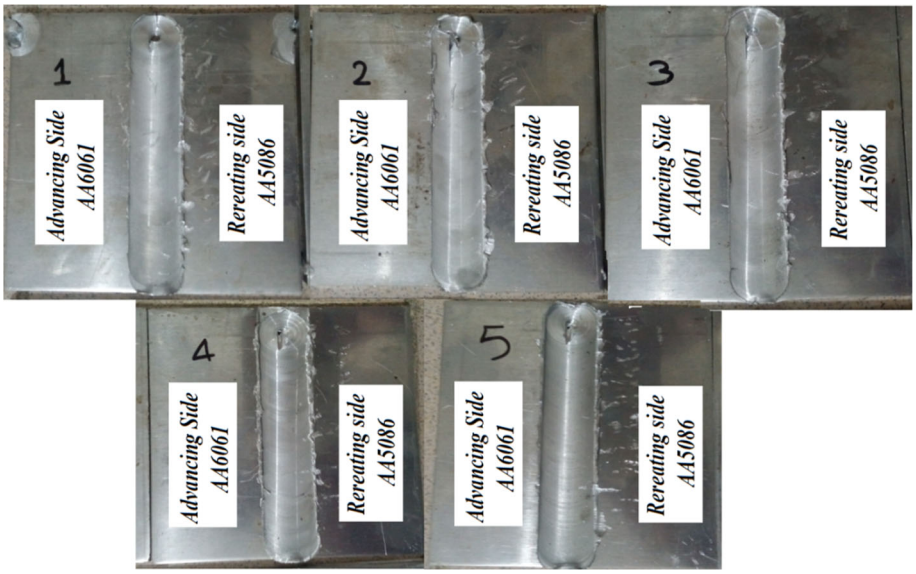

Fig. 4 Welded specimens with different tools

experimental ones. Geometrical modeling of tools was performed by data given in Table 2. Rotational and travel speed were set 840 rpm and 150 mm/min, respectively. It should be mentioned that workpieces specimen, tools dimensions, and FSW parameters were considered as experimental values. In simulation, only welding step was modeled, and tool penetration and retracting stage were not modeled. Elastic and thermal properties of two alloys have been illustrated in Table 3 as functions of temperature.

To model the plastic flow, Johnson-Cook's relation has been used (Johnson & Cook, 1985):

$$\sigma = \left(A + B\varepsilon_p^n\right)\left[1 + C\ \ln\frac{\dot{\varepsilon}_p}{\dot{\varepsilon}_0}\right]\left[1 - \left(\frac{T - T_r}{T_m - T_r}\right)^m\right] \quad (1)$$

Where σ,ε_p, $\dot{\varepsilon}_p$, and $\dot{\varepsilon}_0$ are the yield stress, the effective plastic strain, the effective plastic strain rate, and the normalized strain rate, respectively. Also, T, $T_{r,}$ and T_m are the temperature, transfer temperature, and melting temperature, respectively. A, B, C, $n_{,}$ and m are the constants of the material. These values for AA6061 and AA5086 are illustrated in Table 4.

Table 3 Mechanical and thermal properties of AA6061 and AA5086 alloys (Aval et al., 2011)

Material	Temperature °C	Density Kg/m^3	Young's modulus GPa	Thermal conductivity W/m °C	Heat capacity J/Kg °C	Thermal expansion 10^{-6}/°C
AA6061	25	2700	68.5	167	896	23.4
	100		66.1	180	978	24.6
	150		63.1	184	1004	25.6
	200		59.1	192	1028	26.6
	250		54	201	1052	27.5
	300		46.4	207	1078	28.5
	450		31.7	230	1133	30.7
AA5086	25	2657	70	127	900	23.8
	200		67.8	151	960	25.5
	300		60.7	154	980	26.8
	400		51	158	1020	28.9
	500		37.4	169	1113	31.5

Table 4 Johnson-Cook's constants for AA6061 and AA5086 (Al-Badour et al., 2014)

	A (MPa)	B (MPa)	n	m	C	T_{melt} (K)
AA6061	324	114	0.42	1.34	0.002	856
AA5086	170	425	0.42	1.225	0.0335	913

To simulate the contact interaction between tool and workpieces, general contact technique was utilized and due to literature references, friction coefficient was entered in the ABAQUS software as a function of temperature. The value of this parameter decreases with increasing temperature during the process from 0.4 at room temperature to 0.01 at the melting points of the alloys (Aziz et al., 2016). The tool and workpieces were modeled as Lagrangian and Eulerian, respectively, and the mesh size was selected 1 mm. Tool and workpieces had 2165 number of C3D8T and 75000 number of EC3D8RT elements, respectively.

To verify the numerical model, five numerical achieved maximum temperatures were compared with experimental ones, which have been illustrated in Table 5. For example, temperature distribution contour of specimen number 1 (welded with tool A) and comparative plot for numerical and experimental temperature history of specimen number 4 (welded with tool D) have been shown in Figs. 5 and 6, respectively.

Design of experiments (DOE)

After verification of the numerical model, design of experiments used in this paper is explained. In current research, two quantitative variables named tool offset and pin offset and one qualitative variable known as the position of alloys were considered as inputs, and the maximum temperature in process was considered as output. It should be mentioned that maximum temperature in FSW process was gained at weld line and bottom of tool shoulder. One cannot record this temperature by conventional thermometers or thermocouples. Therefore, numerical models were used to predict the maximum temperatures.

To study the main effects and interactions, Central Composite Design (CCD) was utilized. To use this method and perform analysis of variance (ANOVA), the MINITAB software was used. Each of quantitative variables was considered in five levels, and qualitative variable was assumed to be in two levels. In Table 6, input variables and their levels have been illustrated.

The positive sign indicates the tool offset to the advancing side. Twenty six numerical simulations were performed due to CCD. At each stage of numerical simulation, in order to derive the problem response (maximum process temperature), the mean temperature of 10 welding step frames was used to increase the reliability of the results.

Results and discussion

Model and responses

To study the effect of main factors and interactions on maximum temperature of process, CCD was utilized. Complete second order polynomial was considered for maximum temperature, and design matrix was developed as shown in Table 7. Also in Table 7, the output variables (maximum temperatures) have been illustrated.

In statistical studies, R-squared and adjusted R-squared determine the accuracy of obtained polynomial, which the closer values to unity of mentioned parameters are more accurate. The statistical values of these parameters have been illustrated in Table 8.

The value of reliability factor was chosen as 95%, and ANOVA was utilized which is illustrated in Table 9. The effectiveness of each variable was checked by its *P* value, which should be lower than 5% due to reliability factor

Table 5 Comparison of numerical and experimental maximum recorded temperature

Tool	Maximum temperature (°C)	
	Experimental	Simulation
Tool A	415	411
Tool B	408	407
Tool C	387	391
Tool D	356	363
Tool E	318	309

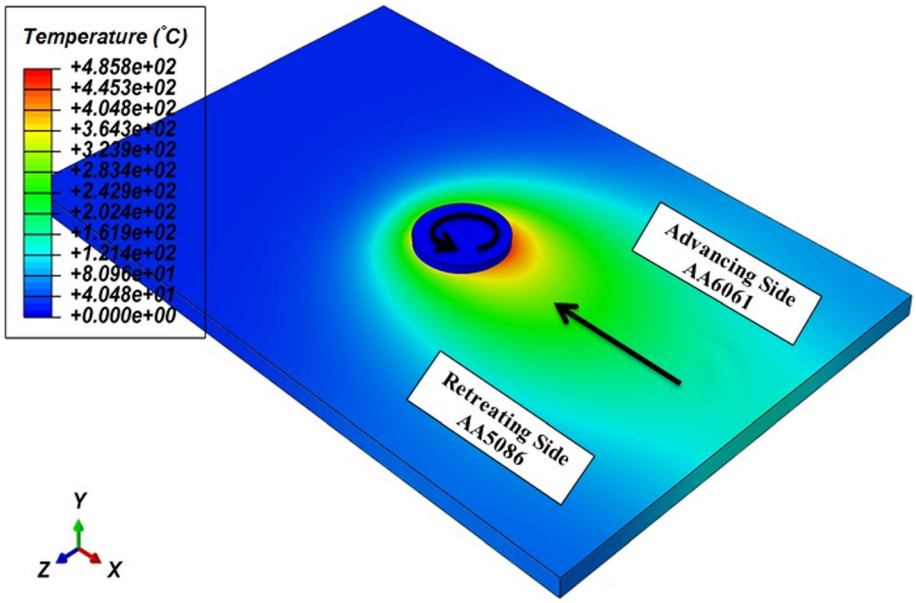

Fig. 5 Temperature contour used for verification (welded with tool A)

of 95%. Based on P values illustrated in Table 9, the coefficients were chosen. Normality of data, stability of variances in different levels, and independency of data from time were checked to verify the fitted model.

The final regression equations of maximum temperature in FSW as a function of considered variables have been illustrated in Table 10 for two cases of locating AA6061 in either advancing or retreating side.

Main effects and interactions

Based on the ANOVA and relations illustrated in Table 10, all the variables directly affect the maximum temperature. Based on the F value and P value shown in Table 9, between three main variables pin offset and the position of alloys have the most and less effect on maximum temperature, respectively.

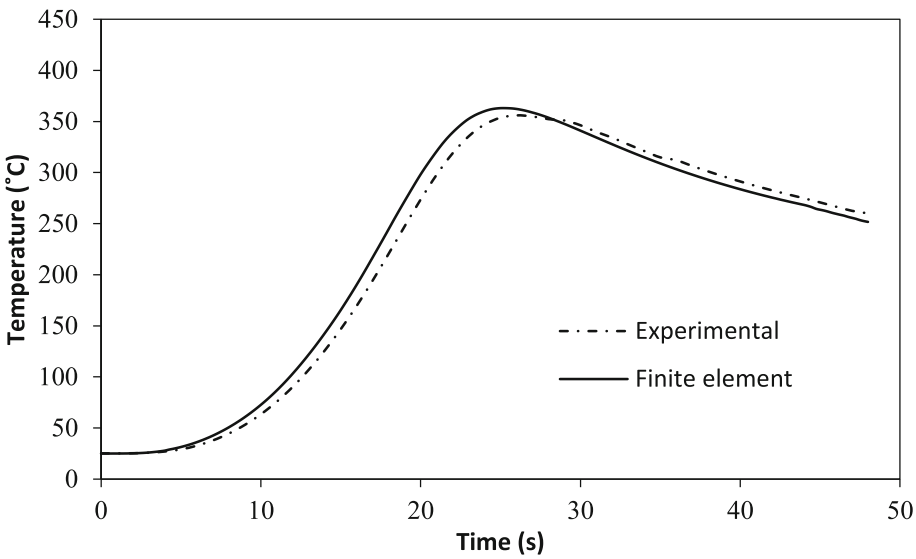

Fig. 6 Numerical and experimental temperature history (welded with tool D)

Table 6 Input variables and their levels

Variables	Unit	Level 1	Level 2	Level 3	Level 4	Level 5
Tool offset	mm	− 2	− 1	0	1	2
Pin offset	mm	0	0.5	1	1.5	2
Position	Advancing side-retreating side	AA6061-AA5086	AA5086-AA6061	–	–	–

The maximum temperature vs pin offset, tool offset, and alloys position have been shown in Figs. 7, 8, and 9, respectively.

Based on the results obtained from Fig. 7, regardless of alloys position, by offsetting the pin, the maximum temperature decreases intensely and by increasing the offset rate, this decrement is more revealed. By offsetting the pin in the constant volume, the plastic flow in a vaster area of workpiece increases. Increasing the pin offsetting causes increment in plastic flow, but results in decrement in plastic flow concentration on central part of welded cross section. Due to this concentration decrement, the heat generated by friction and plastic flow distributes in a vaster area, and the workpieces maximum temperature decreases. In a research

Table 7 Design matrix and output variables

Run order	Tool offset (mm)	Pin offset (mm)	Position advancing side-retreating side	Max temperature (°C)
1	− 1	0.5	AA6061-AA5086	521.8
2	1	0.5	AA6061-AA5086	432.1
3	− 1	1.5	AA6061-AA5086	359.8
4	1	1.5	AA6061-AA5086	333.4
5	− 2	1	AA6061-AA5086	396.7
6	2	1	AA6061-AA5086	312.3
7	0	0	AA6061-AA5086	564.5
8	0	2	AA6061-AA5086	317.3
9	0	1	AA6061-AA5086	428.3
10	0	1	AA6061-AA5086	428.3
11	0	1	AA6061-AA5086	428.3
12	0	1	AA6061-AA5086	428.3
13	0	1	AA6061-AA5086	428.3
14	− 1	0.5	AA5086-AA6061	458.6
15	1	0.5	AA5086-AA6061	414.9
16	− 1	1.5	AA5086-AA6061	351.2
17	1	1.5	AA5086-AA6061	336.6
18	− 2	1	AA5086-AA6061	347.9
19	2	1	AA5086-AA6061	314.5
20	0	0	AA5086-AA6061	475.2
21	0	2	AA5086-AA6061	305.4
22	0	1	AA5086-AA6061	413.5
23	0	1	AA5086-AA6061	413.5
24	0	1	AA5086-AA6061	413.5
25	0	1	AA5086-AA6061	413.5
26	0	1	AA5086-AA6061	413.5

Table 8 The coefficients of statistical model

Source	Std. dev.	R^2	Adjusted R^2	Predicted R^2	PRESS	
Linear	33.06	0.7665	0.7347	0.6212	39017.81	
2FI	32.22	0.8085	0.7481	0.5133	50129.65	
Quadratic	**9.17**	**0.9861**	**0.9796**	**0.9369**	**6500.44**	**Suggested**
Cubic	1.76	0.9996	0.9992	0.9934	675.71	Aliased

performed by Amini et al. (Amini et al., 2015), similar result was obtained.

Based on Fig. 8, tool offsetting toward each advancing or retreating side causes decrement in maximum temperature, which this decrement is more intense while the tool offsetting is toward the advancing side. By tool offsetting, due to unbalance in plastic flow, non-homogeneous and non-uniform flow is generated, and consequently the maximum temperature drops. Due to counter currency of rotational speed and traveling speed in advancing side, lower plastic flow exists rather than retreating side. Therefore, by offsetting the tool toward advancing side, plastic flow decrement occurs more intensely and due to this decrement in material flow, the maximum temperature experiences a larger reduction.

Due to works done by researchers, positioning the dissimilar materials causes major changes in heat distribution, plastic flow of materials, and joint properties. Based on these researches, placing harder material in retreating side causes higher joint mechanical properties (Periyasamy et al., 2018). Some works show vice versa (Zhao et al., 2018). Based on the results obtained from Fig. 9, in all cases, by placing harder alloy in advancing side, the maximum temperature increases than contrariwise placing. Due to unbalance in FSW, the plastic flow forms hardly in advancing side. If harder alloy locates in the advancing side, the transformation of material to plastic phase will take place lower and due to decrement in plastic flow, the maximum temperature will decrease.

Furthermore, interaction of input variables can affect the temperature distribution and maximum temperature. In Fig. 10, the interaction plot of tool offset and pin offset has been shown.

Based on Fig. 10, in low pin offsets by tool offsetting toward each side, the maximum temperature changes have similar pattern. By increasing the pin offset, the amount of temperature drop is different on the two sides of the welding line. Due to presented results, in large pin offsets toward advancing side, the maximum temperature drop is more intensive than retreating side because of harder plastic flow formation. Interaction plots of tool offsetting vs alloys placing and pin offsetting vs alloys placing have been shown in Figs. 11 and 12, respectively.

Due to Fig. 11, tool offsetting, in the case which harder alloy is placed in advancing side, affects the

Table 9 ANOVA of considered model

Source	Sum of squares	Degree of freedom	Mean square	*F* value	*p* value	
Model	1.02E+05	8	12696.93	151.14	< 0.0001	significant
A-tool offset	7005.19	1	7005.19	83.39	< 0.0001	
B-pin offset	68306.14	1	68306.14	813.08	< 0.0001	
C-position	3640.8	1	3640.8	43.34	< 0.0001	
AB	1066.99	1	1066.99	12.7	0.0024	
AC	1065.73	1	1065.73	12.69	0.0024	
BC	2197.85	1	2197.85	26.16	< 0.0001	
A^2	17402.33	1	17402.33	207.15	< 0.0001	
B^2	78.27	1	78.27	0.9317	0.348	
Residual	1428.16	17	84.01			
Lack of fit	1428.16	9	158.68			
Pure error	0	8	0			
Cor total	1.03E+05	25				

Table 10 Final regression equations of maximum process temperature

Position			Regression equation in decoded units
AA6061-advancing side	Temperature	=	553.61–46.85 A–115.4 B–19.49 A × A–5.23 B × B + 23.10 A × B
AA5086-advancing side	Temperature	=	491.67–33.52 A–77.1 B–19.49 A × A–5.23 B × B + 23.10 A × B

maximum temperature drop more intensely. In vice versa situation, maximum temperature drop is smoother because of decrement in plastic flow and energy. Similar to previous situations and based on Fig. 12, it was shown that by placing harder alloy in advancing side, pin offsetting affects maximum temperature drop more intensely. Based on the obtained results, in all situations, pin offsetting causes maximum temperature drop, and this decrement is more intense when harder alloy is in the advancing side.

Conclusion

In this paper, the experimental and finite elements modeling of FSW of two dissimilar alloys AA6061 and AA5086 were performed, and the effects of pin offset, tool offset, and the position of alloys on the maximum process temperature were studied. To investigate the effects of three mentioned variables on the maximum temperature of process and find their interactions, Response Surface Methodology (RSM) has been used, and following results were obtained:

- Based on ANOVA, pin offset was the most effective variable on maximum temperature. By offsetting the pin, decrement in maximum temperature was observed.
- The order of importance of variables on maximum process temperature is pin offset, tool offset, and position of alloys.
- Offsetting the tool causes decrement in maximum temperature, although this decrement is more intense at advancing side.
- In all pin and tool offsetting, placing the harder alloy at advancing side results in more increment in maximum temperature in comparison with the case which the harder alloy is at the retreating side.

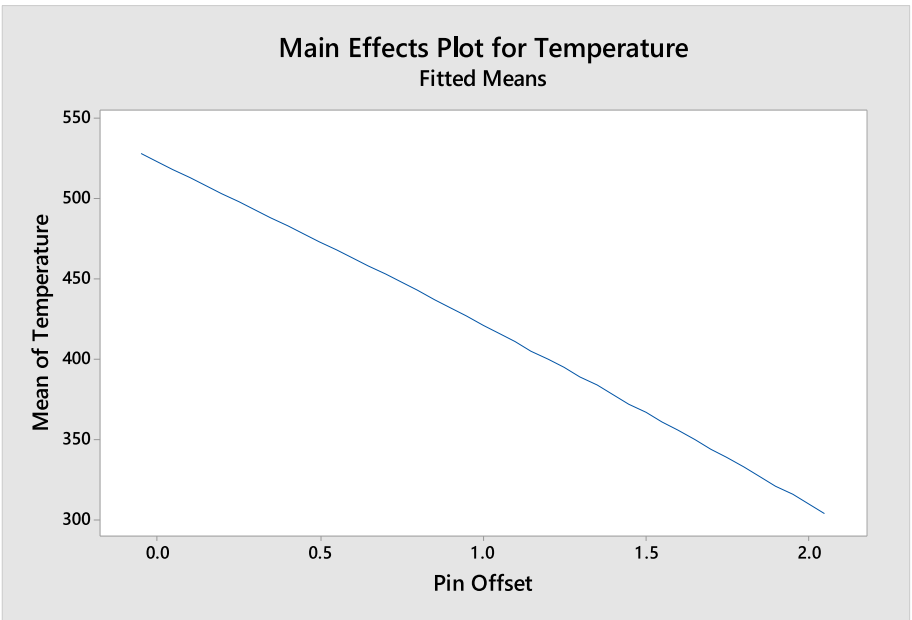

Fig. 7 Main effects plot of pin offset

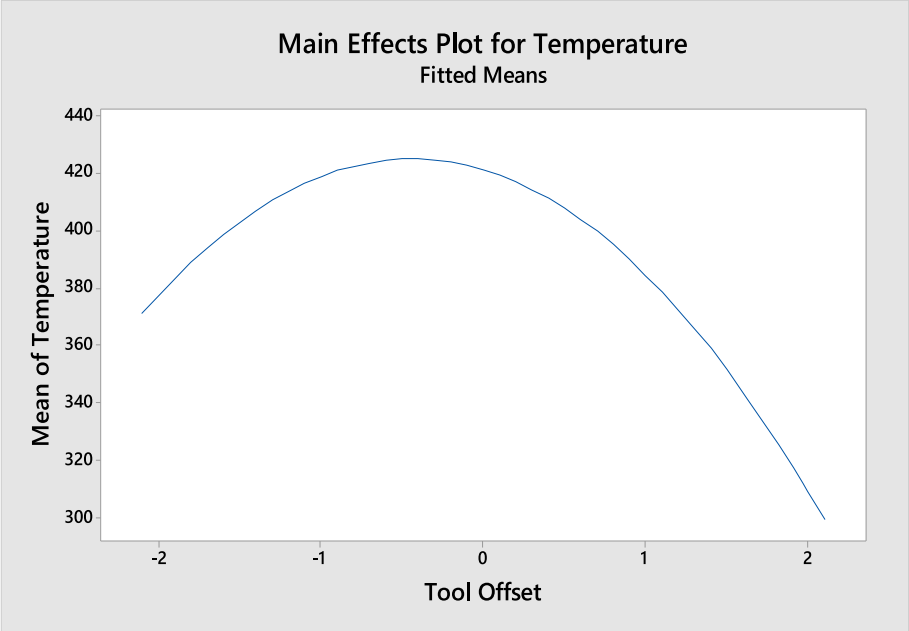

Fig. 8 Main effects plot of tool offset

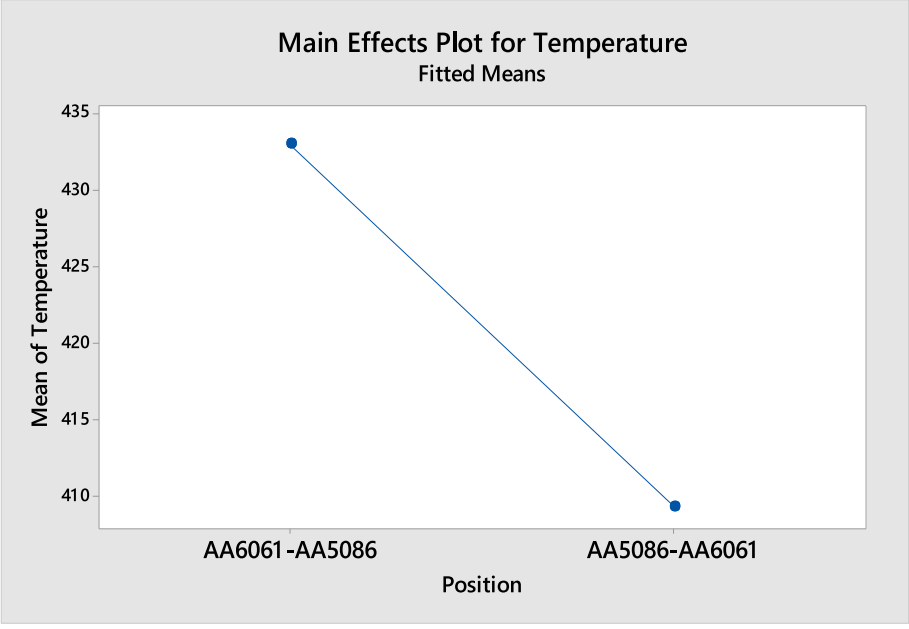

Fig. 9 Main effects plot of alloys position

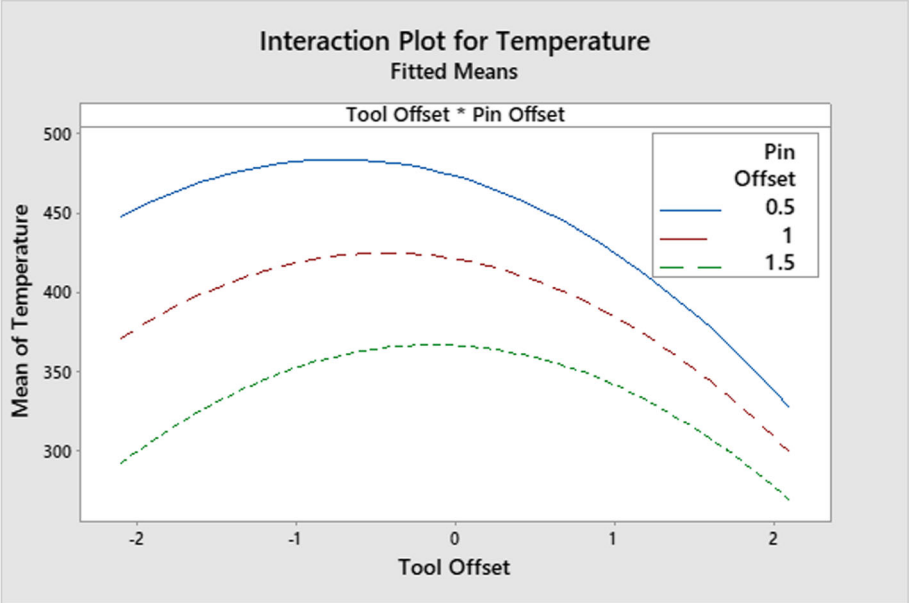

Fig. 10 Interaction plot of tool offset and pin offset on process temperature

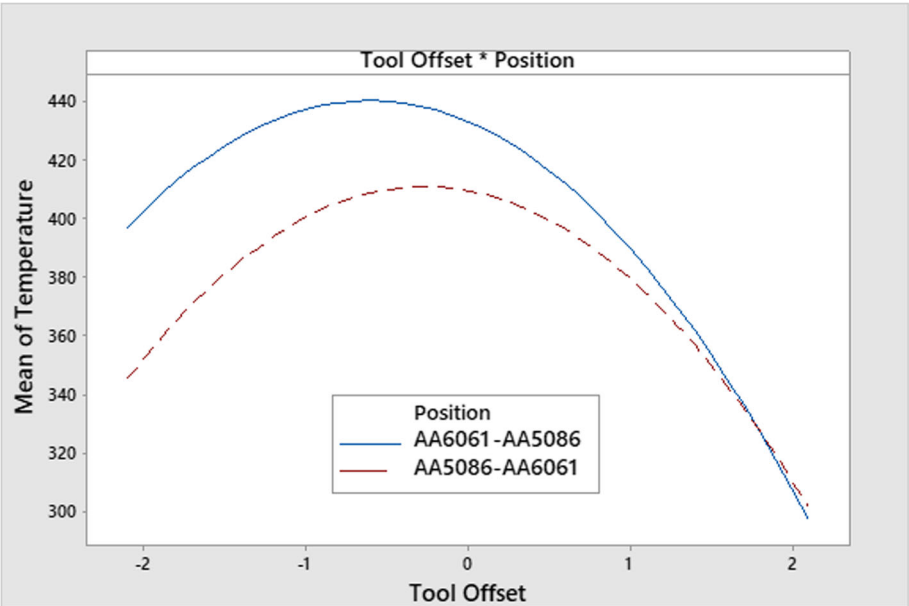

Fig. 11 Interaction plot of tool offsetting vs alloys placing

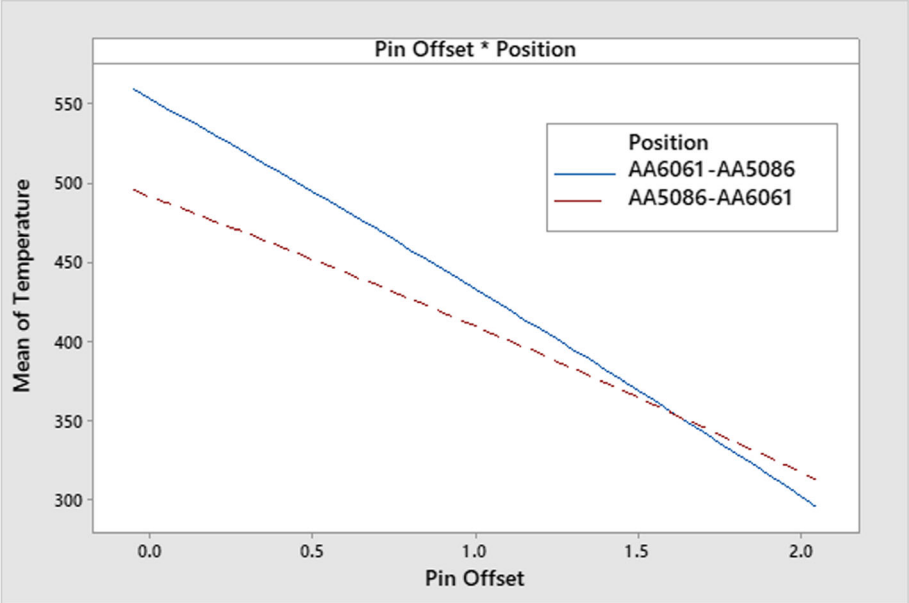

Fig. 12 Interaction plot of pin offsetting vs alloys placing

Abbreviations
FSW: Friction stir welding; RSM: Response Surface Methodology; UTS: Ultimate tensile strength; CCD: Central Composite Design; ANOVA: Analysis of variance

Acknowledgements
Not applicable

Authors' contributions
The authors read and corrected the manuscript. All authors read and approved the final manuscript.

Funding
No specific fund was used for this research.

Availability of data and materials
All data analyzed during this study are available from the corresponding author on request.

Competing interests
The authors declare that they have no competing interests.

Author details
[1]Department of Mechanical Engineering, Tabriz University, Tabriz, Iran. [2]Department of Mechanical Engineering, Faculty of Engineering, Malayer University, Malayer, Iran. [3]Department of Mechanical Engineering, Kermanshah Branch, Islamic Azad University, Kermanshah, Iran.

Received: 28 December 2019 Accepted: 8 May 2020
Published online: 15 May 2020

References

Al-Badour, F., Merah, N., Shuaib, A., et al. (2013). Coupled Eulerian Lagrangian finite element modeling of friction stir welding processes. *Journal of Materials Processing Technology, 213*, 1433–1439.

Al-Badour, F., Merah, N., Shuaib, A., et al. (2014). Thermo-mechanical finite element model of friction stir welding of dissimilar alloys. *The International Journal of Advanced Manufacturing Technology, 72*, 607–617.

Aliha, M., Shahheidari, M., Bisadi, M., et al. (2016). Mechanical and metallurgical properties of dissimilar AA6061-T6 and AA7277-T6 joint made by FSW technique. *The International Journal of Advanced Manufacturing Technology, 86*, 2551–2565.

Amini, S., Amiri, M., & Barani, A. (2015). Investigation of the effect of tool geometry on friction stir welding of 5083-O aluminum alloy. *The International Journal of Advanced Manufacturing Technology, 76*, 255–261.

Aval, H. J., Serajzadeh, S., & Kokabi, A. (2011). Evolution of microstructures and mechanical properties in similar and dissimilar friction stir welding of AA5086 and AA6061. *Materials Science and Engineering: A, 528*, 8071–8083.

Aziz, S. B., Dewan, M. W., Huggett, D. J., et al. (2016). Impact of friction stir welding (FSW) process parameters on thermal modeling and heat generation of aluminum alloy joints. *Acta Metallurgica Sinica (English Letters), 29*, 869–883.

Essa, A. R. S., Ahmed, M. M. Z., Mohamed, A.-K. Y. A., et al. (2016). An analytical model of heat generation for eccentric cylindrical pin in friction stir welding. *Journal of Materials Research and technology, 5*, 234–240.

Johnson, G. R., & Cook, W. H. (1985). Fracture characteristics of three metals subjected to various strains, strain rates, temperatures and pressures. *Engineering fracture mechanics, 21*, 31–48.

Kar, A., Suwas, S., & Kailas, S. V. (2019). Significance of tool offset and copper interlayer during friction stir welding of aluminum to titanium. *The International Journal of Advanced Manufacturing Technology, 100*, 435–443.

Khan, N. Z., Siddiquee, A. N., Khan, Z. A., et al. (2015). Investigations on tunneling and kissing bond defects in FSW joints for dissimilar aluminum alloys. *Journal of Alloys and Compounds, 648*, 360–367.

Liang, Z., Chen, K., Wang, X., et al. (2013). Effect of tool offset and tool rotational speed on enhancing mechanical property of Al/Mg dissimilar FSW joints. *Metallurgical and Materials Transactions A, 44*, 3721–3731.

Mao, Y., Ke, L., Liu, F., et al. (2014). Effect of tool pin eccentricity on microstructure and mechanical properties in friction stir welded 7075 aluminum alloy thick plate. *Materials & Design (1980-2015), 62*, 334–343.

Mastanaiah, P., Sharma, A., & Reddy, G. M. (2016). Dissimilar friction stir welds in AA2219-AA5083 aluminium alloys: effect of process parameters on material inter-mixing, defect formation, and mechanical properties. *Transactions of the Indian Institute of Metals, 69*, 1397–1415.

Mehta, K. P., & Badheka, V. J. (2015). Influence of tool design and process parameters on dissimilar friction stir welding of copper to AA6061-T651 joints. *The International Journal of Advanced Manufacturing Technology, 80*, 2073–2082.

Meyghani, B., Awang, M., Emamian, S. S., et al. (2017). A comparison of different finite element methods in the thermal analysis of friction stir welding (FSW). *Metals, 7*, 450.

Mishra, R. S., De, P. S., & Kumar, N. (2014). *Friction stir welding and processing: science and engineering*. Springer.

Naghibi, H. D., Shakeri, M., & Hosseinzadeh, M. (2016). Neural network and genetic algorithm based modeling and optimization of tensile properties in

FSW of AA 5052 to AISI 304 dissimilar joints. *Transactions of the Indian Institute of Metals, 69*, 891–900.
Pandya SN and Menghani J. 2018. A parametric investigation on effects of friction stir welding process parameters on mechanical properties of AA6061-T6 to Cu dissimilar joints.
Periyasamy, Y. K., Perumal, A. V., & Rajasekaran, D. (2018). Effect of material position and ultrasonic vibration on mechanical behaviour and microstructure of friction stir-welded AA7075-T651 and AA6061 dissimilar joint. *Transactions of the Indian Institute of Metals, 71*, 2575–2591.
Ramachandran, K., Murugan, N., & Kumar, S. S. (2015). Friction stir welding of aluminum alloy AA5052 and HSLA steel. *Welding journal, 94*, 291–300.
Rasaee, S., Mirzaei, A., Almasi, D., et al. (2018). A comprehensive study of parameters effect on mechanical properties of butt friction stir welding in aluminium 5083 and copper. *Transactions of the Indian Institute of Metals, 71*, 1553–1561.
Sahu, P. K., Pal, S., Pal, S. K., et al. (2016). Influence of plate position, tool offset and tool rotational speed on mechanical properties and microstructures of dissimilar Al/Cu friction stir welding joints. *Journal of Materials Processing Technology, 235*, 55–67.
Schmidt, H., Hattel, J., & Wert, J. (2003). An analytical model for the heat generation in friction stir welding. *Modelling and Simulation in Materials Science and Engineering, 12*, 143.
Shah, L., Guo, S., Walbridge, S., et al. (2018). Effect of tool eccentricity on the properties of friction stir welded AA6061 aluminum alloys. *Manufacturing Letters, 15*, 14–17.
Shah, L. H. A., Sonbolestan, S., Midawi, A. R., et al. (2019). Dissimilar friction stir welding of thick plate AA5052-AA6061 aluminum alloys: effects of material positioning and tool eccentricity. *The International Journal of Advanced Manufacturing Technology, 105*, 889–904.
Tamjidy, M., Baharudin, B., Paslar, S., et al. (2017). Multi-objective optimization of friction stir welding process parameters of AA6061-T6 and AA7075-T6 using a biogeography based optimization algorithm. *Materials, 10*, 533.
Yaduwanshi, D., Bag, S., & Pal, S. (2018). On the effect of tool offset in hybrid-FSW of copper-aluminium alloy. *Materials and Manufacturing Processes, 33*, 277–287.
Zhao, Z., Liang, H., Zhao, Y., et al. (2018). Effect of exchanging advancing and retreating side materials on mechanical properties and electrochemical corrosion resistance of dissimilar 6013-T4 and 7003 aluminum alloys FSW joints. *Journal of Materials Engineering and Performance, 27*, 1777–1783.

Publisher's Note